# Jumping crystals of the spinels $NiCr_2O_4$ and $CuCr_2O_4$

**Olivier Crottaz,*[a] Frank Kubel[b] and Hans Schmid[a]**

[a]*Department of Inorganic, Analytical and Applied Chemistry, University of Geneva, 30 Quai Ernest Ansermet, CH-1211 Geneva 4, Switzerland*

[b]*Department of Physical Chemistry, University of Geneva, 30 Quai Ernest Ansermet, CH-1211 Geneva 4, Switzerland*

The crystal structures of cubic and tetragonal $NiCr_2O_4$ and of tetragonal $CuCr_2O_4$ have been refined and their cell parameters have been measured, using single-crystal and powder X-ray diffraction. It has been observed that the differences in the Jahn–Teller distortions in both compounds are reflected in their $M^{2+}-O$ tetrahedral environments and in their cell parameters. A calculation of the atomic shifts during the tetragonal–cubic phase transition showed that the average shifts for the oxygen atoms are 0.10(1) and 0.04(1) Å for the nickel and chromium atoms, respectively. Crystals of both compounds jump when they go through the phase transition. This behaviour is especially spectacular for $NiCr_2O_4$ since the phase transition takes place at 320 K, this temperature being reached when the crystals are illuminated. A comparison with organic jumping crystals is presented, and characteristics of the chromite crystals are discussed.

Nickel chromite ($NiCr_2O_4$) and copper chromite ($CuCr_2O_4$) crystallize, as do numerous other $A^{2+}B_2{}^{3+}O_4$ compounds, with the spinel structure. The high temperature phases of these two compounds have cubic symmetry (space group $Fd\bar{3}m$[1,2]), while the room-temperature phases are tetragonal (space group $I4_1/amd$[3,4]). The phase transition is of first order[5] and takes place at 320 K for $NiCr_2O_4$[6] and at 854 K for $CuCr_2O_4$[7] (on heating). The distortion from cubic to tetragonal symmetry may be considered to arise because of a Jahn–Teller effect, as explained by Dunitz and Orgel.[8]

Our interest in these compounds was initiated by Cox, who predicted a magnetoelectric effect in $NiCr_2O_4$ and $CuCr_2O_4$.[9] With a view to characterizing the magnetoelectric properties of both compounds, single crystals were prepared. Owing to the highly twinned domain states of the crystals it was not yet possible to make magnetoelectric measurements.[7] However, while looking at $NiCr_2O_4$ crystals under a binocular microscope spectacular jumps of the crystals were observed. This stimulated our curiosity and led us to investigate in more detail the crystal structures and the ferroelastic phase transitions of both compounds. Comparisons with other 'jumping crystals' were also made to explain this unusual behaviour. These results are the subject of the present paper.

## Experimental

### Sample preparation

Crystals of $NiCr_2O_4$ and $CuCr_2O_4$ were prepared by a flux decomposition method. This method uses the decomposition, at 1088 K over 24 h, of a $K_2Cr_2O_7$ flux containing 20 mass% CuO or NiO.[7] Black octahedral crystals with a maximum size of $1\times1\times1$ mm$^3$ were obtained. Powders of $CuCr_2O_4$ and $NiCr_2O_4$ were prepared by decomposition of coprecipitated salts according to the procedure described by Whipple and Wold.[10]

### Single crystal X-ray data collection†

The structure of the cubic phase of $NiCr_2O_4$ was refined on a single crystal using a CAD-4 diffractometer with Cu-Kα radiation. When observing the crystals with a binocular microscope it was found that they undergo the phase transition due to the heating provided by the microscope's light source. With a view to reproducing this behaviour on a diffractometer, a halogen lamp was placed close to the crystal (*ca.* 1 cm). In this way a temperature of $353\pm3$ K could be stabilized during the data collection. The determination of the temperature was made by comparison with the cell parameters of polycrystalline powder. The cell parameter was found to be $a=8.3155(7)$ Å at $T=353\pm3$ K. Standardized atomic positions, isotropic displacement parameters and population parameters are summarized in Table 1, selected interatomic distances and angles are shown in Table 2. The refinement was made using the XTAL 3.2 program system.[11]

### Powder X-ray data collection†

The structures of tetragonal $NiCr_2O_4$ and $CuCr_2O_4$ were refined at 298 K on powders obtained by the coprecipitation method. It was not possible to refine the tetragonal structures on single crystals because of the twinning in the tetragonal phase. Data collections were performed on a Philips diffractometer using Co-Kα radiation. Lattice parameters were found to be $a=5.8369(4)$ Å, $c=8.4301(6)$ Å for $NiCr_2O_4$ and $a=6.03052(14)$ Å, $c=7.78230(21)$ Å for $CuCr_2O_4$. For both structures, standardized atomic positions are given in Tables 3 and 4 and selected interatomic distances and angles in Table 2.

The determination of the cell parameters at different tem-

**Table 1** Fractional atomic coordinates, population factors and equivalent isotropic displacement parameters ($10^4$ Å$^2$) of cubic $NiCr_2O_4$ ($Fd\bar{3}m$) with $a=8.3155(7)$ Å at $T=353\pm3$ K (data from a single crystal; e.s.d.s in parentheses)

| | standardized atomic positions and isotropic displacement parameters | | | | | |
|---|---|---|---|---|---|---|
| | Wyckoff notation | $x$ | $y$ | $z$ | population factor | $U_{iso}$ |
| Ni | 8(b) | 3/8 | 3/8 | 3/8 | 0.98(5) | 98(7) |
| Cr | 8(b) | 3/8 | 3/8 | 3/8 | 0.02(5) | 98(7) |
| Cr | 16(c) | 0 | 0 | 0 | 0.99(2) | 64(7) |
| Ni | 16(c) | 0 | 0 | 0 | 0.01(2) | 64(7) |
| O | 32(e) | 0.2384(4) | 0.2384(4) | 0.2384(4) | 1.0 | 90(1) |

425 reflections, $R=3.7\%$, $R_w=3.5\%$.

---

† Atomic coordinates, thermal parameters, and bond lengths and angles for cubic and tetragonal $NiCr_2O_4$ and for tetragonal $CuCr_2O_4$ have been deposited at Cambridge Crystallographic Data Centre (CCDC). See Information for Authors, *J. Mater. Chem.*, 1997, Issue 1. Any request to the CCDC for this material should quote the full literature citation and the reference number 1145/20.

**Table 2** Selected interatomic distances (Å) and angles (°) for $NiCr_2O_4$ and $CuCr_2O_4$ (e.s.d.s in parentheses)

| | compound | $M^{2+}-O$ | $M^{2+}-Cr$ | $Cr-O$ | $Cr-Cr$ | $O-O$ shortest | $O-O$ |
|---|---|---|---|---|---|---|---|
| interatomic distances | $NiCr_2O_4$ cubic | 1.967(3) | 3.4474(2) | 1.987(3) | 2.9400(2) | 2.667(4) | 2.946(4) |
| | $NiCr_2O_4$ tetragonal | 1.885(13) | 3.4289(2) | 2.012(11) | 2.9185(2) | 2.7806(15) | 2.9247(11) |
| | $CuCr_2O_4$ tetragonal | 1.909(3) | 3.2848(1) | 1.992(5) | 2.8864(1) | 2.699(5) | 2.895(5) |
| | | $O-M^{2+}-O$ | $O-M^{2+}-O$ | $O-Cr-O$ | $O-Cr-O$ | $O-Cr-O$ | |
| bond angles | $NiCr_2O_4$ cubic | 109.5(1) | 109.5(1) | 180.0 | 95.69(14) | 84.31(1) | |
| | $NiCr_2O_4$ tetragonal | 104.9(5) | 111.8(3) | 180.0 | 93.4(4) | 86.6(4) | |
| | $CuCr_2O_4$ tetragonal | 121.48(19) | 103.82(8) | 180.0 | 92.27(15) | 87.73(15) | |

Measurement temperatures were 353 K for cubic $NiCr_2O_4$ and 298 K for tetragonal $NiCr_2O_4$ and tetragonal $CuCr_2O_4$.

**Table 3** Fractional atomic coordinates and equivalent isotropic displacement parameters ($10^4$ Å$^2$) of tetragonal $NiCr_2O_4$ ($I4_1/amd$) with $a=5.8369(4)$ Å and $c=8.4301(6)$ Å at $T=298$ K (data from powder, e.s.d.s in parentheses)

| | standardized atomic positions and isotropic displacement parameters | | | | |
|---|---|---|---|---|---|
| | Wyckoff notation | $x$ | $y$ | $z$ | $U_{iso}$ |
| Ni | 4(b) | 0 | 1/4 | 3/8 | 179(2) |
| Cr | 8(c) | 0 | 0 | 0 | 480(30) |
| O | 16(h) | 0 | 0.506(2) | 0.2387(14) | 310(40) |

Step size 0.05°, 60 s step$^{-1}$, $R_{Bragg}=7.6\%$.

**Table 4** Fractional atomic coordinates and equivalent isotropic displacement parameters ($10^4$ Å$^2$) of tetragonal $CuCr_2O_4$ ($I4_1/amd$) with $a=6.030\,52(14)$ Å and $c=7.782\,30(21)$ Å at $T=298$ K (data from powder, e.s.d.s in parentheses)

| | standardized atomic positions and isotropic displacement parameters | | | | |
|---|---|---|---|---|---|
| | Wyckoff notation | $x$ | $y$ | $z$ | $U_{iso}$ |
| Cu | 4(b) | 0 | 1/4 | 3/8 | 110(4) |
| Cr | 8(c) | 0 | 0 | 0 | 138(6) |
| O | 16(h) | 0 | 0.5262(6) | 0.2551(6) | 190(10) |

Step size 0.04°, 30 s step$^{-1}$, $R_{Bragg}=6.0\%$.

peratures was made on a Huber diffractometer with Cu-K$\alpha_1$ radiation. Silicon was used as internal standard.[12] All refinements on polycrystalline samples were made using the Rietveld DBWS-9006PC program.[13]

## Discussion

### Structure of cubic $NiCr_2O_4$

The spinel structures can be described as an approximately cubic close packing of oxygen ions with the metal ions occupying one eighth of the tetrahedral and one half of the octahedral sites. When the $A^{2+}$ ions occupy the tetrahedral sites and the $B^{3+}$ ions the octahedral sites the structure is said to be a normal spinel. The so-called inverse spinel structure is obtained when the tetrahedral sites are occupied by half of the $B^{3+}$ ions with the other half of the $B^{3+}$ and the $A^{2+}$ ions are distributed over the octahedral sites. Structures with partial inversion are also known. The single-crystal data collection performed on cubic $NiCr_2O_4$ allows refinement of the population parameters of the different sites (see Table 1) confirming that $NiCr_2O_4$ has a normal spinel structure, without partial inversion. The normal spinel structure was expected since $Cr^{3+}$ has a high preference for an octahedral environment.[14] Note that the nickel ions are in a regular tetrahedral environment, as reflected by the value of the O—Ni—O angle (see Table 2).

### Cell parameters of $NiCr_2O_4$ and $CuCr_2O_4$ in the tetragonal phase

Fig. 1 and 2 show the variation of the cell parameters and of the $c/a$ ratios of $NiCr_2O_4$ and $CuCr_2O_4$ between 50 and 350 K. It can be seen that these two compounds exhibit different behaviours. The differences in the variations of lattice parameters with temperature are related, as explained by Dunitz

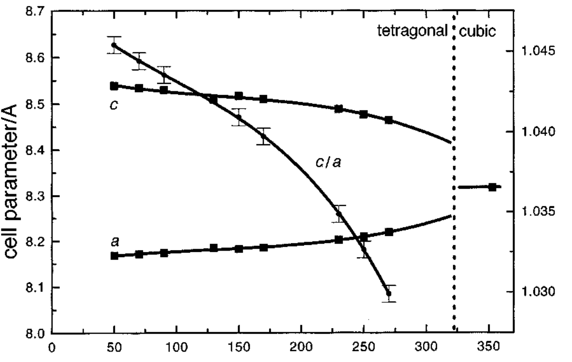

**Fig. 1** Cell parameters and $c/a$ ratio of tetragonal $NiCr_2O_4$ as a function of temperature (squares and error bars correspond to *ca.* $3\sigma$)

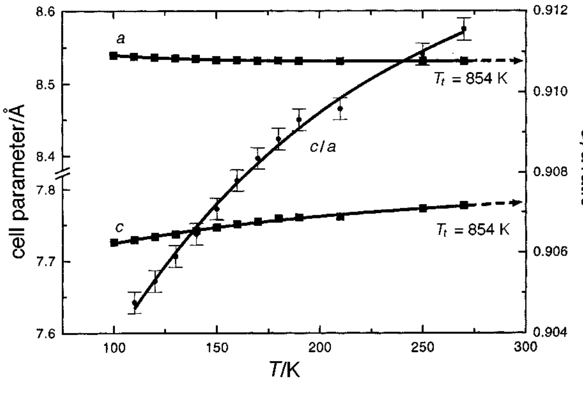

**Fig. 2** Cell parameters and $c/a$ ratio of tetragonal $CuCr_2O_4$ as a function of temperature (squares and error bars correspond to *ca.* $3\sigma$)

and Orgel,[8] to the difference between the Jahn–Teller distortions of tetrahedrally coordinated $Ni^{2+}$ and $Cu^{2+}$ ions [no Jahn–Teller effect is expected for $Cr^{3+}$ ($3d^3$) in an octahedral field].

For $Ni^{2+}$ ($3d^8$) the orbital degeneracy is removed by elongating the tetrahedron along the *c* axis. As a consequence the $d_{xy}$ orbital is stabilized and the $d_{xz}$ and $d_{yz}$ orbitals are destabilized (see ref. 8). In this case the $c/a$ ratio is $> 1.0$ and tends to 1.0 as the temperature is raised. The magnitude of elongation of the tetrahedron can be seen by looking at the O—Ni—O angles listed in Table 2, compared with 109.5(1)° of the perfect tetrahedron observed in the cubic phase.

For $Cu^{2+}$ ($3d^9$) the opposite situation is observed. The orbital degeneracy is removed by compressing the tetrahedron along the *c* axis. This stabilizes the $d_{xz}$ and $d_{yz}$ orbitals at the expense of the $d_{xy}$ orbital (see ref. 8). Therefore the $c/a$ ratio is $< 1.0$ and, as the temperature is raised, $c/a$ tends to 1.0. The O—Cu—O angles listed in Table 2 reflect the magnitude of the deformation.

### Atomic shifts during the phase transition in $NiCr_2O_4$

Since both the cubic and tetragonal structures of $NiCr_2O_4$ have been refined, it was possible to study the shifts of the atoms during the phase transition. However, in order to represent the atoms of both phases on the same frame of reference, it is necessary to turn one of the structures by 45° and to shift its origin. The rotation of the structure was made using the 'Newcell' subroutine of the XTAL 3.2 program.[11] Both structures are then superposed with the 'Rigidbody' subroutine of the XTAL 3.2 program and atomic shifts are calculated. The values of atomic shifts obtained show that the oxygen atoms undergo greater shifts than the chromium and nickel atoms [the average displacement is 0.10(2) Å for the oxygen and 0.04(1) Å for the chromium and nickel atoms]. Fig. 3 shows the displacements of the nickel and oxygen atoms when they undergo the cubic to tetragonal phase transition. The elongation of the Ni—O tetrahedron, discussed above, is visible.

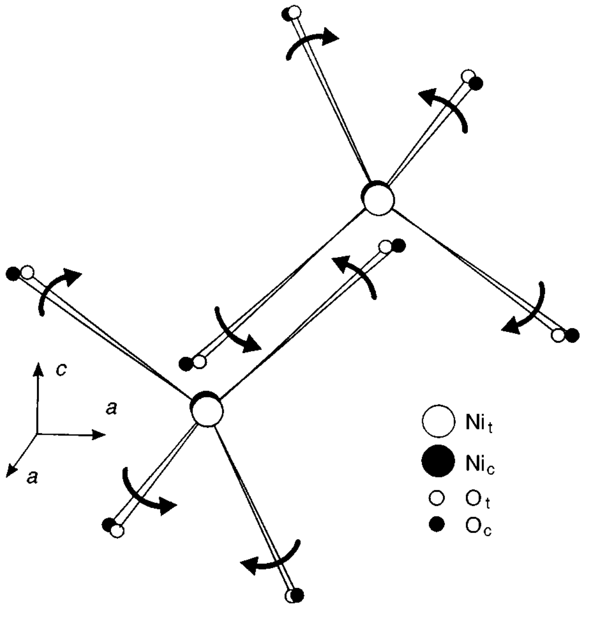

**Fig. 3** Shifts of oxygen and nickel atoms in two $NiO_4^{2-}$ tetrahedra during the phase transition in $NiCr_2O_4$. The arrows show the direction of the atomic shifts during the cubic to tetragonal phase transition.

### Jumping properties

When $NiCr_2O_4$ single crystals were illuminated (for example with the lamp of a binocular microscope), spectacular jumps of the crystals were observed. During these jumps the crystals move horizontally up to 4 mm. When no more movements occurred, the light was turned off and the crystals began to jump again. This behaviour is due to the fact that the heat provided by the light source is sufficient for the $NiCr_2O_4$ crystals to be heated slightly above the tetragonal to cubic phase transition temperature. This is facilitated because the phase transition temperature (320 K) is near to room temperature and the crystals are black (hence strongly absorbing) and relatively small. When the light is turned off the crystals cool and again undergo the phase transition. This cycle was repeated several times without damaging the crystals. It must be said that, contrary to observations reported for organic jumping crystals (see below), the jumps observed are mostly horizontal rather than vertical.

Similar observations can be made for $CuCr_2O_4$. For this compound the phase transition temperature is 854 K.[6] The crystals were placed in a Leitz 1350 heating stage. When the temperature reached the phase transition temperature, crystal jumps were observed. When no more jumps were observed, the temperature was lowered and the crystals began jumping again. Jumps were also observed on $(100)_c$ $CuCr_2O_4$ platelets prepared by polishing. However, after some cycles the platelets broke into smaller pieces.[7]

Jumping properties have been reported already for some organic compounds.[15–18] The jumps observed on these compounds were attributed to mechanical effects, due to unit cell dimension changes[16] or to shifts between different layers of the structure.[15] In Table 5, the unit-cell dimensions of jumping crystals for which unit-cell data were available for both phases are listed. An extensively studied compound for which no jumping effect has been reported is also included for comparison ($BaTiO_3$ was chosen for this purpose because one of its phase transitions is also from tetragonal to cubic symmetry). It can be seen that the jumping crystals show a great discontinuous variation of their cell parameters during the phase transition. The relative change in the cell parameters is as high as 12% for inositol, but much less for copper and nickel chromite (4.5% and −1.36% respectively). This may explain why the inositol crystals jump 'several centimetres high'[17] while the chromite crystals are displaced by some millimetres only. The smaller value of relative change found for $BaTiO_3$ agrees

**Table 5** Unit-cell data of jumping crystals (except $BaTiO_3$) in the low temperature (LT) and high temperature (HT) phases

| compound | $a_{LT}$/Å | $b_{LT}$/Å | $c_{LT}$/Å | $a_{HT}$/Å | $b_{HT}$/Å | $c_{HT}$/Å | $\Delta a_{rel}$ (%) | $\Delta b_{rel}$ (%) | $\Delta c_{rel}$ (%) |
|---|---|---|---|---|---|---|---|---|---|
| oxitropium | 7.388(2) | 10.118 | 24.705 | 7.479(9) | 11.254 | 22.890 | 1.23 | 11.22 | −7.34 |
| inositol | 14.464(6) | 14.923(5) | 16.385(6) | 16.241(8) | 15.230(8) | 14.385(7) | 12.28 | 2.06 | −11.43 |
| $NiCr_2O_4$ | 5.8369(4) |  | 8.4301(6) | 8.3155(7) |  |  | 0.73 |  | −1.36 |
| $CuCr_2O_4$ | 6.016(4) |  | 7.981(4) | 8.344(2) |  |  | −1.93 |  | 4.55 |
| $BaTiO_3$ | 3.999 |  | 4.030 | 4.010 |  |  | 0.28 |  | −0.50 |

Measurement temperature for the cell parameters: for $NiCr_2O_4$, 298 K and 353 K; for $CuCr_2O_4$, 840 K and 855 K; for inositol, 333 K and 353 K, for oxitropium 293 K and 348 K; for $BaTiO_3$, 360 K and 410 K. Δ refers to the low-temperature–high temperature phase transition. Space groups for oxitropium are $P2_1/c$ for both phases with $\beta = 89.61°$ (LT) and 73.52° (LT). Space groups for inositol are $P2_12_12_1$ for both phases with $\beta = 103.21(1)°$ (LT) and 96.73(4)° (HT). Data for $CuCr_2O_4$ are from ref. 1, for oxitropium from ref. 16, for inositol from ref. 17 and for $BaTiO_3$ from ref. 19.

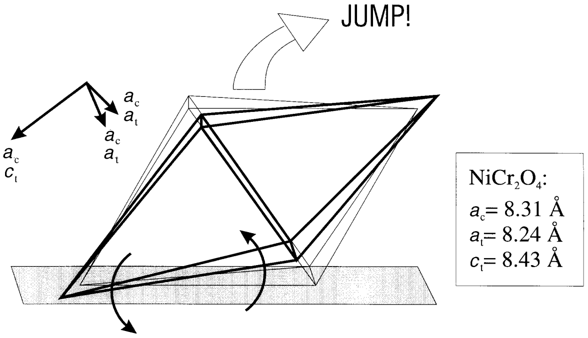

**Fig. 4** Modifications of the dimensions of an $NiCr_2O_4$ octahedron lying on a $(111)_c$ facet during the phase transition. Dimensions in the cubic phase are shown as thin lines, those in the tetragonal phase as bold lines. The arrows show the modifications perpendicular to the $(111)_c$ facet during the cubic to tetragonal phase transition.

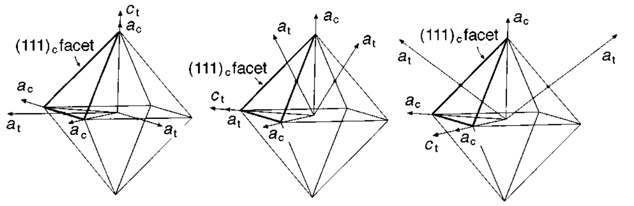

**Fig. 5** Orientations of the crystallographic axes in the three ferroelastic domains of tetragonal $NiCr_2O_4$ (or $CuCr_2O_4$) with respect to the morphology of the crystal

with the fact that no jumps have so far been reported for this compound.

When trying to explain the jumps in chromite crystals, some of their characteristics must be taken into consideration. First, the chromite crystals have an octahedral morphology with only $(111)_c$ natural facets and before the phase transition the crystals are lying on these facets. Secondly, no change of space group occurs during the phase transition in the organic crystals. This implies that no domains are generated at the transition, while the phase transition in the chromites is a ferroic one with different high-temperature and low-temperature point groups leading to the formation of three equivalent domain states in the tetragonal phase.[7] Consequently, the magnitude of the jumps of the chromites is governed mainly by the relative change in length perpendicular to the $(111)_c$ facets, for each of the three domains.

In Fig. 4 the modification of (unit cell) dimensions perpendicular to one $(111)_c$ facet of a single domain $NiCr_2O_4$ crystal during the cubic to tetragonal phase transition is shown. It can be seen that the resulting impulsion (represented by dark arrows in Fig. 4) takes place near the apex of the octahedron and is not purely vertical, which is in agreement with the displacements observed. During the tetragonal to cubic phase transition the impulsions on Fig. 4 are inverted, the impulsion taking place near the central plane of the octahedron. The same considerations also apply to $CuCr_2O_4$. However, the dimension changes are inverted with respect to $NiCr_2O_4$, since for $CuCr_2O_4$ $a_t\sqrt{2} > a_c > c_t$.

Fig. 5 shows the orientation of the crystallographic axes with respect to the morphology of the crystal for the three possible domain orientations. Note that the three different domains are related by a three-fold axis perpendicular to the $(111)_c$ facet with each type of domain having its $c_t$ axis pointing towards one apex of the octahedron. Consequently, during the cubic to tetragonal phase transition each domain will give its own impulsion in a plane perpendicular to the $(111)_c$ facet, thus giving polydomain crystals the possibility to jump. As before the impulsion's locations are inverted in the tetragonal to cubic transition, but each domain also gives a contribution perpendicularly to the $(111)_c$ facet.

The considerations discussed in the two previous paragraphs only for $NiCr_2O_4$ also apply to $CuCr_2O_4$; however, the dimension changes are inverted since for $CuCr_2O_4$ $a_t\sqrt{2} > a_c > c_t$.

It should be noted that another possibility to explain the jumps observed would be to consider potential attraction–repulsion between crystals. However, this explanation disagrees with the fact that jumps also occur when only one crystal is observed. Moreover, the creation of charges during the phase transition is not expected, since both structures are found to be centrosymmetric.

## Conclusions

Crystals and powders of $NiCr_2O_4$ and $CuCr_2O_4$ have been prepared and the crystal structures of the cubic and tetragonal phases have been refined. The different Jahn–Teller distortions for both compounds are reflected in the different temperature dependence of the cell parameters and $O-M^{2+}-O$ angles. The jumps observed for both compounds, when they undergo the tetragonal to cubic phase transition both upon heating and cooling, can be attributed to the large changes in the (unit-cell) dimensions occurring during the ferroelastic phase transition. Note that the 'jumping effect' is also induced by the Jahn–Teller effect: the jumps are due to modifications of the dimensions of the crystal which are the result of atomic displacements occurring during the phase transition as a consequence of a Jahn–Teller distortion. Possible applications of $NiCr_2O_4$ as a light or heat sensitive micromechanical device may be imagined.

The authors wish to express their gratitude to the Swiss National Science Foundation for support.

### References

1 V. M. Ust'yantsev and V. P. Mar'evich, *Inorg. Mater.*, 1974, **9**, 306.
2 E. J. W. Verwey and E. L. Heilmann, *J. Chem. Phys.*, 1947, **15**, 174.
3 F. Bertaut and C. Delorme, *C. R. Acad. Sci.* (*Paris*), 1954, **239**, 505.
4 E. Prince, *J. Appl. Phys.*, 1961, **32**, 68.
5 P. Pausescu and R. Manaila, *Sov. Phys. Crystallogr.*, 1969, **13**, 533.
6 T. Armbruster, G. A. Lager, J. Ihringer, F. J. Rotella and J.-D. Jorgensen, *Z. Kristallogr.*, 1983, **162**, 8.
7 Z. G. Ye, O. Crottaz, F. Vaudano, F. Kubel. P. Tissot and H. Schmid, *Ferroelectrics*, 1994, **162**, 103.
8 J. D. Dunitz and L. E. Orgel, *J. Phys. Chem. Solids*, 1957, **3**, 20.
9 D. E. Cox, *Int. J. Magnetism*, 1974, **6**, 67.
10 E. Whipple and A. Wold, *J. Inorg. Nucl. Chem.*, 1962, **24**, 23.
11 *XTAL 3.2 Reference Manual*, ed. S. R. Hall, H. D. Flack and J. M. Stewart, Universities of Western Australia, Geneva and Maryland, 1992.
12 D. N. Batchelder and R. O. Simmons, *J. Chem. Phys.*, 1964, **41**, 2324.
13 D. B. Wiles and R. A. Young, *J. Appl. Crystallogr.*, 1981, **14**, 149.
14 J. D. Dunitz and L. E. Orgel, *J. Phys. Chem. Solids*, 1957, **3**, 318.
15 J. Ding, R. Herbst, K. Praefcke, B. Kohne and W. Saenger, *Acta Crystallogr., Sect. B*, 1991, **47**, 739.
16 S. Zamir, J. Bernstein and D. J. Greenwood, *Mol. Cryst. Liq. Cryst.*, 1994, **242**, 193.
17 T. Steiner, W. Hinrichs, W. Saenger and R. Gigg, *Acta Crystallogr., Sect. B*, 1993, **49**, 708.
18 J. Gigg, R. Gigg, S. Payne and R. Conant, *J. Chem Soc., Perkin Trans. 1*, 1987, 2411.
19 L. A. Shebanov, *Phys. Status Solidi A*, 1981, **65**, 321.

*Paper* 6/04758K; *Received* 8*th July*, 1996